1 # Combined Impacts of ENSO and MJO on the 2015 Growing
2 # Season Drought over the Canadian Prairies

3   Zhenhua Li[1,2], Yanping Li[1], Barrie Bonsal[3], Alan H. Manson[2] ,Lucia Scaff[1]

4   [1]Global Institute for Water Security, University of Saskatchewan, Saskatoon, Saskatchewan, Canada S7N3H5

5   [2]Institute of Space and Atmospheric Studies, University of Saskatchewan, Saskatoon, Saskatchewan, Canada

6   [3]National Hydrology Research Center, Environment and Climate Change Canada, Saskatoon, SK, Canada

7   *Correspondence to*: Dr. Yanping Li (yanping.li@usask.ca); Dr. Zhenhua Li (zhenhua.li@usask.ca)

8   **Abstract**

9   Warm-season precipitation over the Canadian Prairies plays a crucial role in activities in environment and society

10   and has particular importance to agricultural production over the region. This research investigates how a warm season

11   precipitation deficit over the Canadian Prairies is related to tropical Pacific forcing in the early summer 2015 drought. The

12   significant deficit of precipitation in May and June of 2015 were coincident with a warm phase of El Nino-Southern

13   Oscillation (ENSO) and a negative phase of Madden-Julian Oscillation (MJO)-4 index as they both favor a positive

14   geopotential height anomaly in western Canada. Further investigation during the instrumental record period (1979-2015)

15   shows that the warm-season precipitation in the Canadian Prairies and the corresponding atmospheric circulation anomalies

16   over western Canada teleconnected with the lower boundary conditions in the tropical western Pacific. MJO may play a

17   crucial role in determining the summer precipitation anomaly in the western Canadian Prairie when equatorial central Pacific

18   is warmer than normal (NINO4 > 0) and MJO is more active. The mechanism of this teleconnection may be due to the

19   propagation of stationary Rossby wave that is generated in the MJO-4 index region. When the tropical convection around

20   MJO-4 index regions (western tropical Pacific, centered over 140 E) is more active than normal when NINO4 >0, a Rossby

21   wave train originates from western Pacific and propagates into the midlatitude North America causing an anomalous ridge in

22   the upper level over western Canada.

23 # 1 Introduction

24   The Canadian Prairies are highly dependent on summer precipitation especially during the early

25   to mid-growing season (May through July) when the majority of annual precipitation normally occurs

26 (Bonsal et al. 1993). High natural variability in growing season precipitation causes periodic

27 occurrences of extreme precipitation (Li et al. 2017) and droughts that are often associated with reduced

28 agriculture yields, low stream flow, and increased occurrence of forest fires (Wheaton et al. 2005,

29 Bonsal and Regier 2007). Drought events with great environmental and economic impacts have

30 occurred in 1961, 1988, 2001-2002, and as recent as 2015 (Dey 1982, Liu et al. 2004, Bonsal et al.

31 1999, Wheaton et al. 2005, Shabbar et al. 2011, Bonsal et al. 2013, Szeto et al. 2016). The sub-seasonal

32 forecasting of precipitation during the growing season are crucial for the agriculture, water resource

33 management, and the economy in the region. Therefore, an investigation into the potential causes of the

34 inter-annual variability of growing season precipitation of the Canadian Prairie is much needed to

35 provide important information for the agriculture and economy in the region.

36 Low precipitation and extended dry periods on the Canadian Prairies are often associated with

37 upper-level ridge and a persistent high pressure centered over the Prairies (Dey 1982, Liu et al. 2004).

38 These prolonged atmospheric anomalies often concurred with abnormal boundary conditions such as

39 large-scale sea surface temperature (SST) anomalies in the Pacific (Shabbar and Skinner 2004). Large

40 scale oscillation in the SST anomalies in Pacific Ocean, namely El Nino, the Pacific Deccadal

41 Oscillation (PDO), can affect the hydroclimatic pattern in North America, although the strongest

42 impacts of these boundary conditions occur during the boreal winter. Inter-annual variabilities such as

43 El Nino-Southern Oscillation (ENSO) events are found to be linked with extended droughts in the

44 Prairies (Bonsal et al. 1999, Shabbar and Skinner 2004). Interdecadal oscillation such as the PDO, and

45 the Atlantic Multi-decadal Oscillation (AMO) have also been found to affect the seasonal temperature

46 and precipitation in the Canadian Prairies (Shabbar et al. 2011).

47 ENSO's relationship with the Canadian Prairies' precipitation has been studied extensively. The

48 warm phase of ENSO often favours drought in the Canadian Prairies, especially during the growing

49 season after the mature phase of El Nino with North Pacific Mode (NPM) like North Pacific SST

50   anomaly pattern (Bonsal and Lawford 1999, Shabbar and Skinner 2004). Previous investigations (e.g.,

51   Shabbar *et al.* (2011)) have found El Nino events are associated with a summer moisture deficit in the

52   western Canada while La Nina events cause an abundance of moisture in extreme western Canada

53   (British Columbia and Yukon). However, they also noted that although tropical SST variability

54   accounted for some aspects of the large-scale circulation anomalies that influence Canadian Prairies

55   drought, a consistent and clear-cut relationship was not found. North Pacific SST warm anomalies,

56   which often follow a matured El Nino, and accompanying atmospheric ridging leads to extended dry

57   spells over the Prairies during the growing season (Bonsal and Lawford 1999). For the recent North

58   Pacific SST anomaly from 2013 to 2014, researchers have attributed the precipitation deficit in

59   California during 2013 to the anomalous upper-level ridge over the western North America (Wang *et al*.

60   2014, Szeto et al. 2016).

61   The formerly mentioned SST variations (ENSO, PDO, etc.) mostly vary on interannual and

62   decadal scales. Another important factor that affects the weather patterns in North America is the

63   Madden-Julian Oscillation (MJO), an intra-seasonal (40-90 days) oscillation in convection and

64   precipitation pattern in the Tropics (Zhang 2005, Madden and Julian 1971, Riddle *et al.* 2013, Carbone

65   and Li 2015). MJO is a coupled atmosphere-ocean oscillation involving convections and large-scale

66   equatorial waves, which produces an eastward movement of tropical convection anomaly on an

67   intraseasonal scale (Madden and Julian 1971). MJO has been found to affect the winter temperature and

68   precipitation in North America and Europe through its impact on moisture transport associated with

69   "Pineapple Express" and its effects on North Atlantic Oscillation and stratospheric polar vortex (Cassou

70   2008, Garfinkel *et al.* 2012, Rodney et al. 2013). MJO has been found to be connected to precipitation

71   anomalies to summer precipitation in the Southwest United States (Lorenz and Hartmann 2006). During

72   spring and summer, MJO's impact on the Canadian Prairies' precipitation has not been thoroughly

73   investigated as MJO's amplitude is weak during summer. The amplitude of MJO in spring and early

74   summer, however, is related to the interannual variation of tropical SST, especially the SST in central

75   Pacific (Hendon et al. 2007, Marshall et al. 2016). The amplitude of MJO in terms of the Real-time

76   Multivariate MJO index (RMM, Wheeler and Hendon 2004) was extremely strong in the early spring of

77   2015 with high SST anomaly in the central Pacific and El Nino became strong.

78   MJO activities in the western Pacific under the modulation of interannual variability of SST have

79   the potential to act together and impact mid-tropospheric circulation over western Canada and thus,

80   warm season precipitation over the Canadian Prairies. The goal of the study is to demonstrate that the

81   mechanism involved MJO may cause the meteorological drought in growing season in the Canadian

82   Prairies in 2015. Subsequently, further investigations are carried out to determine if similar relationships

83   exist in association with other summer extreme precipitation events during instrumental record (1979-

84   2016). Section 2 provides the datasets and methodologies used in this paper while section 3 presents

85   analyses of the upper-level circulation anomaly and SST pattern associated with the 2015 drought. This

86   is followed by examination of the effects of central Pacific SST anomaly and MJO on the summer

87   precipitation in the Canadian Prairies using data during instrumental record period.The potential

88   mechanism by which MJOaffects summer precipitation when equatorial central Pacific SST is warmer

89   than normal is discussed in section 4 followed by a summary of the results and concluding remarks in

90   section 5.

91   2 Data and Methodology

92   2.1 Data

93

94   Multiple observation and reanalysis datasets are used to investigate the circulation anomalies

95   associated with Canadian Prairie growing season (May-August) precipitation. Observed precipitation is

96   taken from the Climate Prediction Center (CPC) Merged Analysis of Precipitation (CMAP) dataset (Xie

97   and Arkin 1997). Geopotential height fields include those from the National Center for Environmental

98   Predictions (NCEP) Reanalysis (Kalnay *et al.* 1996) and the European Center for Medium-Range

99   Weather Forecast (ECMWF)'s ERA-interim (Dee *et al.* 2011), and are used to analyze upper-level (200

100   hPa and 500 hPa) atmospheric circulation patterns.

101   To represent the central Pacific SST anomaly, NINO4 SST index (Rayner et al. 2003) from CPC

102   of National Oceanic and Atmospheric Administration (NOAA) is used since the NINO4 region is near

103   central Pacific and spans over the dateline (5°S-5°N, 160°E-150°W). Multivariate ENSO Index (MEI)

104   data are retrieved from National Oceanic and Atmospheric Administration (NOAA)'s Climate Data

105   Center (CDC) website and are used to determine the ENSO phase (Wolter 1987, Wolter and Timlin

106   1993). In particular, an El Nino condition is defined when the monthly mean index of MEI is larger than

107   0.5 as it identifies El Nino events consistently (Andrews et al. 2004).

108   The Real-time Multivariate MJO series (RMM1 and RMM2) developed by Wheeler and Hendon

109   (2004) are used to identified the periods of strong MJO activities as the MJO amplitudes are readily

110   available by the calculation of the square root of RMM1 + RMM2. For MJO intensities in a region, we

111   used the monthly averaged pentad MJO indices from NOAA CPC's MJO index (Xue *et al.* 2002) which

112   have 10 indices representing locations around the globe. The CPC's MJO index is based on Extended

113   Empirical Orthogonal Function (EEOF) analysis on pentad velocity potential at 200-hPa. Ten daily MJO

114   indices are constructed by projecting the daily (00Z) velocity potential anomalies at 200-hPa (CHI200)

115   onto the ten time-lagged patterns of the first EEOF of pentad CHI200 anomalies (Xue *et al.* 2002).

116   Negative values of ten MJO indices correspond to enhanced convections to 10 regions centered on

117   20°E, 70°E, 80°E, 100°E, 120°E, 140°E, 160°E, 120°W, 40°W and 10°W in the tropics. A negative

118   value of the CPC's MJO indices (usually varies between -2 to 2) indicates an above average convective

119   activities in the corresponding region. Because boreal summer corresponds to a period of weaker

120   amplitude of MJO than winter, we choose monthly mean value of -0.3 as the criterion of strong

121   convections that are connected to MJO. The monthly mean MJO-4 index less than -0.3 is the criterion

122   considered as a relatively strong convection associated with MJO in the western Pacific where has been

123   found to be a source region of stationary Rossby waves (Simmons 1980). SST observations include

124   Extended Reconstructed Sea Surface Temperature (ERSST) v4 (Huang *et al.* 2015). Outward Longwave

125   Radiation (OLR) data from NOAA Interpolated Outgoing Longwave Radiation (hosted at

126   http://www.esrl.noaa.gov/psd/map/clim/olr.shtml) are used to derived the composite anomalous field of

127   OLR for a certain phase of MJO as described below.

128

129

3 Results

131   This study focuses on the growing season precipitation in the provinces of Alberta and Saskatchewan in

132   the Canadian Prairies, where the largest deficits were observed in 2015. Specifically, the regional mean

133   precipitation over 115°-102.5°W, 50°-57.5°N is used (boxed arear in Figure 1) to represent the

134   Canadian Prairies east of the Rocky Mountains and south of the boreal forest. The region chosen also

135   covers most of the arable land in the Canadian Prairies for datasets with 2.5-degree resolution. As the

136   indicated by the MJO-4 and NINO4 index for 2015, the relationship between the Prairies' warm season

137   (May-August) precipitation with MJO-4 and ENSO during the instrumental records are investigated

138   using correlation and regression. The possible mechanism behind the correlation between MJO-4 and

139   the Prairie's warm season precipitation during El Nino condition is further investigation by analyzing

140   the upper-level circulation associated with convections in the Tropics and stationary Rossby waves in

141   the midlatitudes.

142

3.1 The 2015 Summer Drought

Almost all of western Canada including British Columbia, the southern Northwest Territories, Alberta and Saskatchewan had significant negative precipitation anomalies during May and June 2015. The warm season precipitation is represented by the monthly mean precipitation from May to August (Bonsal *et al*. 1999, Shabbar *et al*. 2011). For the 2015 case study, during May-June, the prairies' precipitation was significantly below average. The top plot in Fig. 1 shows the precipitation anomaly in percentage relative to climatology (1981-2010 long term mean) in Canada during May and June 2015. The bottom plot in Fig. 1 presents the monthly precipitation anomaly averaged over the region encompassed by the dash lines (50N-57.5N, 115W-102.5W). The annual cycle of the regional precipitation has, in average, a dry period between February and May. Regarding the precipitation climatology, June has the largest precipitation in all months with significantly more rain than neighboring months. When both May and June 2015 witness much less precipitation than normal in addition to a relatively dry period from February to April, the region gets little precipitation.

Fig. 1 Top: Precipitation anomalies (mm) from CMAP over the region (115 W-102.5 W, 50 N-57.5 N) during May and June 2015. Bottom: time series of monthly precipitation anomaly over boxed region between September 2013 and August 2015.

The upper-level geopotential height anomaly averaged in May and June are examined together with SST anomaly and ENSO, MJO-4 indices for 2014 and 2015. The 500 hPa geopotential height (GPH) anomaly for the May and June 2015 shows strong positive anomalies near Alaska and British Columbia coast in Fig. 2, which is consistent with the findings for other growing season droughts (e.g., Dey 1982; Bonsal and Wheaton, 2005). Accompanying this anomalous ridge extending from Alaska to Pacific Northwest of the US is an above normal warm SST in the northeast Pacific off the coast of North America and the central-eastern Pacific (Fig. 3). Both ENSO and North Pacific Mode (NPM) (Hartmann et al. 2015) are in positive phases that corresponds to a warmer SST near the Pacific coast of North

167   America, consistent with the positive GPH anomalies in western Canada and Alaska. The ridge in

168   Alaska/Bering Straits and the one near British Columbia coast are associated with El Nino and North

169   Pacific SST anomaly such as NPM (Shabbar *et al.* 2011). The monthly mean anomalous ridge indicates

170   a tendency to prevent storms from reaching the British Columbia coast and the Canadian Prairies

171   causing extended dry spells. The GPH anomaly in early growing season in 2015 is consistent with the

172   precipitation anomaly in these regions. The anomalous upper-level ridge in the Western United States

173   and Canada in 2014 and 2015 have also been associated with the developing El Nino and the other main

174   components of Pacific sea surface temperature (SST) variation such as NPM by several recent studies

175   (Hartmann 2015, Lee *et al*. 2015, Li et al. 2017).

176   Fig. 2 NCEP GPH anomaly at 500hPa during May and June 2015 when the precipitation deficit was the largest.

177   Fig. 3 shows the average SST anomaly during the growing season (May-August) of 2015. The

178   strong positive anomaly in the Northeast Pacific and eastern equatorial Pacific is evident and persistent

179   through the summer, which corresponds to the warm phase of NPM and ENSO, respectively. SST in the

180   eastern tropical Pacific warms increasingly since the end of 2014 and qualifies as an El Nino in early

181   2015. The NPM becomes positive since fall 2013 and turns to exceptionally strong in 2014 and persist

182   to 2015 (Hartmann 2015). The anomalous ridge is concurrent with strong SST anomalies in both

183   tropical Pacific and extratropical North Pacific. NPM, as the third EOF of Pacific SST (30S-65N), also

184   has a strong connection to the anomalous ridge in the western North America and trough in the eastern

185   US and Canada in 2013-2014 winter (Hartmann 2015, Lee *et al.* 2015). During the ENSO-neutral

186   condition in 2013 and 2014, the precursor of ENSO, so-called "footprinting" mechanism is considered

187   by some researchers to cause this anomalous ridge in the western North America (Wang *et al.* 2014).

188   Summer of 2015 is the first summer after the developing El Nino during 2014-2015 winter.

189   Though the upper-level GPH pattern seen in summer 2015 can be attributed to the SST modes in the

190   Pacific Basin, namely ENSO and NPM, the precipitation in the Western Canadian Prairie is not strongly

191   correlated with either of them. Bonsal and Lawford (1999) found that more extended dry spells tend to

192   occur during the second summer following the mature stage of the El Nino events. The winter

193   precipitation in Canada has been shown to have a strong connection to ENSO (Shabbar et al. 1997),

194   whereas summer precipitations in most regions of western Canada (except the coast of British Columbia

195   and Southern Alberta) do not have significant correlations with ENSO. This is consistent with our

196   investigation using instrumental records from 1948 to 2016.

197   The variation of the Canadian Prairies' precipitation and its relationship with SST modes and

198   MJOs shown in Fig. 4. The time series of monthly RMM amplitude anomaly, NINO4 index, MJO-4

199   indices and the Canadian Prairies precipitation anomaly from January 2014 to December 2015 shows

200   the atmospheric-oceanic circulation condition for the drought in 2015. In 2015 both May and June saw a

201   strong MJO-4 negative indices, whereas in July the MJO-4 index became positive. This corresponds

202   quite well with the precipitation anomaly in Fig. 1. As shown in Fig. 3, the 0El Nino continued to

203   strengthen in July and August 2015; in the meantime, the MJO-4 index increased in July and August

204   2015. The increase of MJO-4 index corresponded to the active convections associated with MJO in

205   West Pacific propagated eastward into the central Pacific; the precipitation in the Canadian Prairie

206   returned to slightly above normal in July.

207   The good correspondence of MJO-4 index and negative precipitation anomaly suggests a link

208   between MJO related tropical convection anomaly and the prairie precipitation during growing season.

209   Though El Nino and associated Northeast Pacific warm anomaly (i.e., NPM) in summer 2015 can be a

210   contributing factor for the upper-level ridge on the west coast of Canada, it cannot fully explain the

211   drought condition in West Canada as these SST conditions does not guarantee a prolonged dry spell as

212   shown by correlation analysis. The negative MJO-4 index concurred with the negative anomaly of

213   Prairie precipitation in 2015, which prompts the investigation of their relationship in the instrumental

214   records.

215   Fig. 3 The mean SST anomaly(ºC) from ERSST v4 in May-August 2015.

216   Fig. 4 RMM amplitude anomaly, NINO4, MJO 4 indices and precipitation anomaly of Canadian Prairies from January 2014

217   to Dec 2015.

218

219   3.2 Instrumental record

220   El Nino and its associated North Pacific SST anomaly may contribute to extended dry spells in

221   Canadian Prairies after the matured phase of El Nino (Bonsal et al. 1993) on an interannual time scale.

222   ENSO, however, is not a strong intra-seasonal to seasonal predictor of Canadian Prairie summer

223   precipitation. Here we present a new result showing that under warm central Pacific SST condition

224   (NINO4 >0), a certain phase of MJO, which connected to the active convections in the tropical western

225   Pacific (Li and Carbone 2012), plays an important role to determine the precipitation in the Canadian

226   Prairies in the early summer months.

227   Table 1 Correlation between mean precipitation anomaly from CMAP in the prairie and MEI, MJO indices 4. MJO

228   indices and are from 1979 to 2016. CMAP covers 1979 to 2016.

229

230   The correlation coefficients between the mean regional precipitation anomaly over Canadian

231   Prairies and MJO-4 indices and MEI from May to August are shown in Table 1. The correlation

232   between MEI and the precipitation anomalies is not significant. The negative MJO-4 index represents a

233   stronger than normal convection in the Maritime Continents and the tropical Western Pacific. The

234   correlation between MJO-4 index and precipitation in the Prairies indicates that stronger tropical

235   convections in the Equatorial region centered around 140ºE favor less precipitation in the Canadian

236   Prairies from May to August. The correlation between MJO-4 index and the growing season Prairie

237   precipitation anomaly is 0.18 with a p-value of 0.023. The correlation between MJO-4 index and the

238   precipitation anomaly during growing season when NINO4 >0 is much higher at 0.33 with a p-value of

239   0.0015. The correlation between MJO-4 and the Canadian Prairie precipitation when NINO4 < 0 is -

240   0.01.

241   Fig. 5 The scatterplot of monthly precipitation anomaly (mm/month) as a function of MJO-4 and NINO4. Each

242   asterisk represents a month from May to August 1979-2016. Circled asterisk denotes a month with precipitation anomaly

243   larger than 18 mm/month. The blue circles are months with positive precipitation anomaly and the red circles are months with

244   negative precipitation anomaly. The sizes of circles denote the magnitudes of the anomalies (large > 30 mm/month, medium >

245   24 mm/month, small >18 mm/month). The shaded area denotes NINO4>0 and MJO-4 index < 0.

246   The scatter plot in Fig. 5 shows the distribution of monthly precipitation anomaly versus MJO-4

247   index and NINO4 index, which together affect the precipitation anomaly from May to August. Circled

248   asterisk denotes a month with precipitation anomaly larger than 18 mm/month and the red (blue) circles

249   denote negative (positive) precipitation. The sizes of the circle represent the magnitude of the monthly

250   precipitation anomalies. In the bottom-right region indicated by shading, under NINO4 > 0 condition,

251   negative MJO-4 corresponds to many more dry months than wet months. We noticed that some

252   significant dry months are not in the shaded region which corresponds to the dry months occur in La

253   Nina condition or in the period after the mature phase of El Nino (Bonsal et al. 1999).

254   Fig. 6 The box-percentile plot of Canadian Prairies precipitation anomaly during growing season for ENSO

255   conditions.

256   To investigate the impact of ENSO on the growing season precipitaiton over Canadian Prairies,

257   the distribution of precipitation anomaly along ENSO conditions are plotted. The box-percentile plot in

258   Fig. 6 shows the distribution of monthly Canadian Prairies' precipitation anomalies from May to August

259   along ENSO condition. In general, under El Nino and ENSO neutral condition the precipitation

260   anomalies centered on 0, and there is no bias toward either end. Under La Nina condition, the mean

261   precipitation has a positive bias. There are only 10 summer months under La Nina condition, whereas

262   both El Nino and neutral condition have 71 months.

263   The distributions of precipitation anomalies versus MJO-4 index under different ENSO

264   conditions are shown in Fig. 7. Under warm central Pacific SST condition (NINO4 >0), the precipitation

265   anomaly has a negative tendency for MJO-4 < -0.3. Under NINO4 >0 condition, there is no such

266   negative tendency for the precipitation anomaly under the condition of MJO-4 < -0.3. Based on Fig. 6

267   and 7, the significant correlation between precipitation and MJO-4 under NINO4 > 0 condition relative

268   to ENSO in Table 1 is demonstrated in detail.

269   Fig. 7 Box-percentile plots of Canadian Prairies' precipitation anomaly during growing season versus MJO-4 under

270   warm NINO4 (NINO4> 0, left) and cold NINO4 (NINO4<0, right) condition.

271   The strong correlation between MJO-4 and the prairie precipitation during growing season leads

272   us to investigate the underlying circulation anomalies. Fig. 8 presents the regressed stream function and

273   wind field at 200 hPa in the midlatitudes (north of 30N) on the negative MJO-4 index from May to

274   August under warm NINO4 SST condition (NINO4 > 0.). In the tropics (10S-20N, considering it is

275   during Northern Hemisphere summer), the OLR, velocity potential, and divergent wind vector are

276   plotted. Only regression patterns have p-values lower than 0.05 are plotted for OLR and velocity

277   potential. The negative MJO-4 index corresponds to a negative anomaly in OLR, stronger convection

278   and larger than average divergence in the region centered on 150 E. The strong convection anomaly

279   centers on 150 E, 5 N with divergent wind extending well into the subtropics in the Northern

280   Hemisphere. The positive GPH/stream function anomaly extended from Japan to central Pacific is

281   associated with the enhanced convection and divergence in the upper troposphere over the western

282   tropical-subtropical Pacific. A Rossby wave train linked to the OLR anomaly and strong divergence in

283   the western Pacific propagate eastward into North America.

4 Discussion

284

285   The growing season precipitation in the Canadian Prairies are affected by many factors and

286   precipitation deficit can occur under various circulation and lower boundary conditions. Thus it is not

287   expected to find a universal condition for all the significant droughts in the region. In fact, extreme

288   drought conditions have been found in both El Nino years and La Nina years. Though previous research

289   by Bonsal and Lawford (1999) indicates the meteorological drought often occurs after the mature phase

290   of El Nino, which is not the case for 2015, the associated changes in the North Pacific represented by

291   NPM positive phase is consistent with their results. The direct linkage between ENSO and the summer

292   precipitation in the Canadian Prairies is still not clear. In fact, the correlation between MEI and

293   precipitation in the investigated region is -0.096 (p=0.2389, sample size = 152). It is not a significant

294   correlation which is consistent with other researchers' findings (Dai and Wigley 2000).

295   The regression pattern is consistent with stationary Rossby wave theory as shown in a hierarchy

296   of theoretical and modeling studies (Karoly *et al.* 1989, Simmons *et al.* 1983, Hoskins and Ambrizzi

297   1993, Ambrizzi and Hoskins 1997, Held *et al.* 2002). A similar wave train extends from the western

298   Pacific toward South America in the extratropics but at lower latitudes compared to its counterpart in the

299   Northern Hemisphere (not shown). The node of the wave train in Western Canada and Northwest

300   Pacific of the US corresponds to an anomalous ridge, which is in-phase of El Nino forcing. When the

301   convection in the region associated with MJO-4 is weaker than normal (MJO-4 > 0), a wave train with

302   the opposite sign would reach western Canada which would counteract on El Nino forcing. Thus, the

303   weak correlation between Canadian Prairie precipitation and ENSO is understandable as MJO plays an

304   additional role that enhances or cancels out the GPH anomaly caused by El Nino.

305   The atmospheric response in midlatitude North America to the tropical forcing in the western

306   Pacific depends on the mean circulation condition associated with tropical SST. Intraseasonal tropical

307   convection oscillation in the western Pacific associated with MJO-4 index cannot determine the sign of

308   precipitation anomaly in the prairie. Both warm SST in central Pacific and strong tropical convection in

309   western Pacific and Maritime Continent are necessary to cause a significant precipitation deficit in the

310   western Canadian Prairies. Warm SST in central Pacific causes an eastward expansion of Pacific warm

311   pool that favors enhanced MJO activity in the western-central Pacific (Hendon et al. 1999, Marshall et

312   al. 2016). For the year of 2015, while the anomalous positive GPH associated with strong negative

313   MJO4 indices in addition to the SST anomaly in the Pacific (e.g. ENSO, NPM) forced the anomalous

314   ridge on the west coast of Canada which reduces precipitation in the Canadian Prairies in the early

315   summer. Although the El Nino continued to strengthen in July and August 2015, the active convections

316   associated with MJO in West Pacific propagated eastward into the central Pacific, as the convection in

317   the western Pacific/Maritime Continent waned, the precipitation in the Canadian Prairie returned to

318   slightly above normal in July.

319   Fig. 8 The regression of stream function, wind field in the extratropics on MJO-4 for May-August with MEI > 0.5.

320   Bottom: OLR, velocity potential, and divergent wind in the tropics on MJO-4 indices for May-August with $NINO4 > 0$. The

321   shaded region for the tropical OLR has p-value < 0.05. Blue shading indicates active convection region. Red dashed contour

322   and solid blue contour corresponds to negative and positive velocity potential, respectively.

323   5 Conclusions

324   The cause of the summer precipitation deficit in the western Canadian Prairies is investigated

325   regarding atmospheric circulation anomalies, sea surface temperature, and intraseasonal tropical

326   convection oscillation, MJO. The drought in western Canada is immediately related to the anomalous

327   ridge in the upper-level. The persistent anomalous upper-level ridge hovering around the west coast of

328   Canada and Alaska since fall 2014 is likely associated with SST anomaly in the tropical (ENSO) and

329   extratropical Pacific (NPM) as both SST patterns tend to associate with an anomalous high in Alaska

330   and western Canada. However, the anomalous ridge itself explains the drought in the western Canada,

331   the underlying cause of the anomalous ridge and whether it is related to ENSO need investigation . After

332 all the significant deficit of precipitation concentrated in May and June 2015 when El Nino was still

333 growing in intensity. The correlation of ENSO with the prairie precipitation is also not significant during

334 summer. Instead, the intraseasonal oscillation in tropical convection, MJO, plays an important role in

335 determining precipitation anomaly during months with warm central Pacific SST (NINO4 > 0).

336   In general, MJO-4 indices demonstrate significant correlation with the meteorological drought

337 from May to August with warm SST in central Pacific (NINO4 >0) when MJO amplitude is also often

338 stronger. The new finding in our investigation is that MJO phase/strength is connected to the anomalous

339 ridge in Western Canada when NINO4 is positive through the propagation of stationary Rossby wave

340 from the western Pacific. The connection between the Canadian Prairie precipitation deficit and MJO is

341 stronger when NINO4 is positive because MJO amplitude is stronger when the central Pacific SST is

342 warmer than normal (NINO4 >0). The underlying cause of this significant correlation between MJO-4

343 indices and the prairie precipitation in May-August is a stationary Rossby wave train originates from

344 Maritime Continent and western Pacific and propagate into Canada. The intra-seasonal predictability in

345 MJO amplitude and phase can be potentially instrumental for medium-range/intra-seasonal projection of

346 the growing season precipitation in the Canadian Prairies when the central-Pacific SST is warm.

347

348   Acknowledgement

349 We gratefully acknowledge the Natural Sciences and Engineering Research Council of Canada

350 (NSERC) for funding the Changing Cold Regions Network (CCRN) through their Climate Change and

351 Atmospheric Research (CCAR) Initiative. Dr. Zhenhua Li is supported by the Probing the Atmosphere

352 of the High Artic project sponsored by the NSERC. This research is also supported by Environment and

353 Climate Change Canada (ECCC). Dr. Y. Li gratefully acknowledges the support from the Global

354 Institute of Water Security at the University of Saskatchewan.

References

355

356 Ambrizzi T and Hoskins B J 1997: Stationary Rossby-Wave Propagation in a Baroclinic Atmosphere,

357 *Quart. J. Roy. Meteor. Soc.,* **123** 919–28.

358 Andrews, E.D., R.C. Antweiler, P.J. Neiman, and F.M. Ralph 2004 Influence of ENSO on Flood

359 Frequency along the California Coast. *J. Climate,* **17**, 337–348, doi: 10.1175/1520-0442(2004)017.

360 Bonsal, B.R., Chakravarti, A.K. and Lawford, R.G. 1993: Teleconnections between North Pacific SST

361 Anomalies and Growing Season Extended Dry Spells on the Canadian Prairies, Int. J. Climatol., 13,

362 865-878.

363 Bonsal, B.R., Zhang, X. and Hogg, W.D., 1999: Canadian Prairie growing season precipitation

364 variability and associated atmospheric circulation, *Climate Research*, *11*(3), 191-208.

365 Bonsal B and Lawford R 1999: Teleconnections between El Niño and La Niña Events and Summer

366 Extended Dry Spells on the Canadian Prairies, *International Journal of Climatology,* **19,** 1445–58.

367 Bonsal B R, Shabbar A and Higuchi K, 2001: Impacts of Low Frequency Variability Modes on

368 Canadian Winter Temperature, *Int. J. Climatol.* **21,** 95–108.

369 Bonsal B R and Regier M, 2007: Historical Comparison of the 2001/2002 Drought in the Canadian

370 Prairies, Climate Research, **33**, 229-242.

371 Bonsal, B R, Aider, R, Gachon, P and Lapp S, 2013: An Assessment of Canadian Prairie Drought: Past,

372 Present, and Future, Climate Dynamics, **41**, 501–516.

373 Carbone R. E., Yanping Li, 2015: Tropical Oceanic Rainfall and Sea Surface Temperature Structure:

374 Parsing Causation from Correlation in the MJO, *Journal of Atmospheric Science*, Vol. 72, No. 7, 2703–

375 2718.

376 Cassou C, 2008: Intraseasonal Interaction Between the Madden-Julian Oscillation and the North

377 Atlantic Oscillation, *Nature,* **455** 523–7.

378 Dai A and Wigley T M L, 2000: Global Patterns of ENSO-Induced Precipitation, *Geophys. Res. Lett.,*

379 **27** 1283–6.

380 Dee D P, Uppala S M, Simmons A J, Berrisford P, Poli P, Kobayashi S, Andrae U, Balmaseda M A,

381 Balsamo G, Bauer P, Bechtold P, Beljaars A C M, Berg L van de, Bidlot J, Bormann N, Delsol C,

382 Dragani R, Fuentes M, Geer A J, Haimberger L, Healy S B, Hersbach H, Hólm E V, Isaksen L, Kållberg

383 P, Köhler M, Matricardi M, McNally A P, Monge-Sanz B M, Morcrette J-J, Park B-K, Peubey C,

384 Rosnay P de, Tavolato C, Thépaut J-N, and Vitart F, 2011: The ERA-Interim Reanalysis: Configuration

385 and Performance of the Data Assimilation System, *Quarterly Journal of the Royal Meteorological*

386 *Society,* **137,** 553–97.

387 Dey B, 1982: Nature and Possible Causes of Droughts on the Canadian Prairies-Case Studies, *Journal of*

388 *Climatology,* **2,** 233–49.

389 Garfinkel C I, Feldstein S B, Waugh D W, Yoo C and Lee S, 2012: Observed Connection Between

390 Stratospheric Sudden Warmings and the Madden-Julian Oscillation, *Geophys. Res. Lett.,* **39.**

391 Hartmann D L, 2015: Pacific Sea Surface Temperature and the Winter of 2014, *Geophys. Res. Lett.,* **42,**

392 1894–902.

393 Held I. M., Ting M. and Wang H., 2002: Northern Winter Stationary Waves: Theory and Modeling *J.*

394 *Climate,* **15**, 2125–44.

395 Hendon, H. H., C. Zhang, and J. D. Glick, 1999: Interannual variation of the Madden-Julian Oscillation

396 during Austral summer, J. Clim., 12, 2538–2550

397 Hong, C. C., Hsu, H. H., Tseng, W.-L., Lee, M. Y., Chow, C.-H., & Jiang, L.-C. 2017: Extratropical

398 Forcing Triggered the 2015 Madden–Julian Oscillation–El Niño Event. *Sci. Rep.* **7**, 46692; doi:

399 10.1038/srep46692.Hoskins B J and Ambrizzi T, 1993: Rossby Wave Propagation on a Realistic

400 Longitudinally Varying Flow. *J. Atmos. Sci.* **50** 1661–71

401 Huang B, Banzon V F, Freeman E, Lawrimore J, Liu W, Peterson T C, Smith T M, Thorne P W,

402 Woodruff S D and Zhang H-M, 2015: Extended Reconstructed Sea Surface Temperature Version 4

403 (ERSST. v4). Part I: Upgrades and Intercomparisons *Journal of Climate,* **28** ,911–30.

404   Kalnay E, Kanamitsu M, Kistler R, Collins W, Deaven D, Gandin L, Iredell M, Saha S, White G,

405   Woollen J, Zhu Y, Chelliah M, Ebisuzaki W, Higgins W, Janowiak J, Mo K, Ropelewski C, Wang J,

406   Leetmaa A, Reynolds R, Jenne R and Joseph D, 1996: The NCEP/NCAR 40-Year Reanalysis Project

407   *Bull. Amer. Meteor. Soc.* **77** 437–71

408   Karoly D J, Plumb R A, and Ting M, 1989: Examples of the Horizontal Propagation of Quasi-Stationary

409   Waves. *J. Atmos. Sci.* **46** 2802–11

410   Lee M Y, Hong C C and Hsu H H 2015: Compounding Effects of Warm Sea Surface Temperature and

411   Reduced Sea Ice on the Extreme Circulation Over the Extratropical North Pacific and North America

412   During the 20132014 Boreal winter *Geophys. Res. Lett.,* **42**, 1612–8.

413   Yanping Li, Richard E. Carbone, 2012: Excitation of rainfall over the tropical western Pacific. *Journal*

414   *of Atmospheric Science,* Vol. 69, No. 10, 2983–2994.

415   Yanping Li, Kit Szeto, Ron Stewart, Julie Theriault, Liang Chen, Bob Kochtubajda, Anthony Liu,

416   Sudesh Boodoo, Ron Goodson, Curtis Mooney, Sopan Kurkute, 2017: The June 2013 Alberta

417   Catastrophic Flooding: Water vapor transport analysis by WRF simulation. *Journal of*

418   *Hydrometeorology,* Vol. 18, 2057-2078.

419   Zhenhua Li, Alan Manson, Yanping Li, Chris Meek, 2017: Circulation Characteristics of Persistent

420   Cold Spells in Central-Eastern North America. *Journal of Met. Res.*, Vol. 31, 250-260.

421   Liu J, Stewart R E and Szeto K K, 2004: Moisture Transport and Other Hydrometeorological Features

422   Associated With the Severe 2000/01 Drought Over the Western and Central Canadian Prairies *Journal*

423   *Of Climate,* **17**, 305–19.

424   Lorenz, D.J. and D.L. Hartmann, 2006: The Effect of the MJO on the North American Monsoon. *J.*

425   *Climate,* **19**, 333–343, doi: 10.1175/JCLI3684.1.

426   Madden R A and Julian P R, 1971: Detection of a 40-50 Day Oscillation in the Zonal Wind in the

427   Tropical Pacific, *J. Atmos. Sci.,* **28**, 702–8

428   Marshall, A. G., H. H. Hendon, and G. Wang, 2016: On the role of anomalous ocean surface

429   temperatures for promoting the record Madden-Julian Oscillation in March 2015, Geophys. Res. Lett.,

430   43,472–481.

431   Riddle E E, Stoner M B, Johnson N C, L'Heureux M L, Collins D C and Feldstein S B, 2013: The

432   Impact of the MJO on Clusters of Wintertime Circulation Anomalies Over the North American region

433   *Climate Dynamics,* **40**, 1749–66.

434   Rodney, M., Lin, H., & Derome, J. 2013: Subseasonal Prediction of Wintertime North American

435   Surface Air Temperature during Strong MJO Events. *Monthly Weather Review, 141*(8), 2897–2909.

436   http://doi.org/10.1175/MWR-D-12-00221.1.

437   Ropelewski C F and Halpert M S 1986: North American Precipitation and Temperature Patterns

438   Associated with the El Niño/Southern Oscillation (ENSO), *Monthly Weather Review*, **114**, 2352–62.

439   Shabbar, A., Bonsal, B. and Khandekar, M., 1997: Canadian precipitation patterns associated with the

440   Southern Oscillation. Journal of Climate 10:3016-3027.

441   Shabbar A and Skinner W, 2004: Summer Drought Patterns in Canada and the Relationship to Global

442   Sea Surface Temperatures, *Journal of Climate,* **17**, 2866–80.

443   Shabbar A, Bonsal B R and Szeto K, 2011: Atmospheric and Oceanic Variability Associated with

444   Growing Season Droughts and Pluvials on the Canadian Prairies, *Atmosphere-Ocean,* **49**, 339–55.

445   Simmons A J, Wallace J M and Branstator G W, 1983: Barotropic Wave Propagation and Instability,

446   and Atmospheric Teleconnection Patterns, *J. Atmos. Sci.,* **40**, 1363–92.

447   Szeto, K., X. Zhang, R.E. White, and J. Brimelow, 2016: The 2015 Extreme Drought in Western

448   Canada. *Bull. Amer. Meteor. Soc.,* **97**, S42–S46,https://doi.org/10.1175/BAMS-D-16-0147.1.

449   Wang S Y, Hipps L, Gillies R R and Yoon J-H, 2014: Probable Causes of the Abnormal Ridge

450   Accompanying the 2013-2014, California Drought: ENSO Precursor and Anthropogenic Warming

451   footprint *Geophys. Res. Lett.,* **41** 3220–6.

452   Xie P and Arkin P A, 1997: Global Precipitation: A 17-year Monthly Analysis Based on Gauge

453   Observations, Satellite Estimates, and Numerical Model Outputs. *Bulletin of the American*

454   *Meteorological Society,* **78,** 2539–58.

455   Xue Y, Higgins W and Kousky V 2002: Influences of the Madden-Julian Oscillations on Temperature

456   and Precipitation in North America during ENSO-neutral and Weak ENSO Winters, *Proc. workshop on*

457   *prospects for improved forecasts of weather and short-term climate variability on subseasonal (2 week*

458   *to 2 month) time scales.*

459   Wheaton, E, Wittrock V, Kulshreshtha S, Koshida G, Grant C, Chipanshi A, Bonsal BR, 2005: Lessons

460   Learned from the Drought Years of 2001 and 2002: Synthesis Report. Agriculture and Agri-Food

461   Canada, Saskatchewan Research Council Publ No. 11602–46E03, Saskatoon.

462   Wheeler, M. C., & Hendon, H. H., 2004: An all-season real-time multivariate MJO index: Development

463   of an index for monitoring and prediction. *Monthly Weather Review*, *132*(8), 1917–1932.

464   Wolter, K., 1987: The Southern Oscillation in surface circulation and climate over the tropical

465   Atlantic, Eastern Pacific, and Indian Oceans as captured by cluster analysis. J. Climate Appl.

466   Meteor., 26, 540-558.

467   Wolter, K. and M.S. Timlin, 1993: Monitoring ENSO in COADS with a seasonally adjusted principal

468   component index. Proc. of the 17th Climate Diagnostics Workshop, Norman, OK,

469   NOAA/NMC/CAC, NSSL, Oklahoma Clim. Survey, CIMMS and the School of Meteor., Univ. of

470   Oklahoma, 52-57.

471   Zhang C, 2005: Madden-Julian Oscillation *Reviews of Geophysics,* **43.**

472

473

474

475

476

483

484   Table 1 Correlation between mean precipitation anomaly from CMAP in the prairie and MEI, MJO

485   indices 4. MJO indices and are from 1979 to 2016. CMAP covers 1979 to 2016.

	Correlation	p-value	No. of sample
MEI	-0.096	0.24	156
MJO-4	0.18	0.023	156
MJO-4(NINO4>0)	0.33	0.0015	90
MJO-4(NINO4<0)	-0.01	0.94	66

486
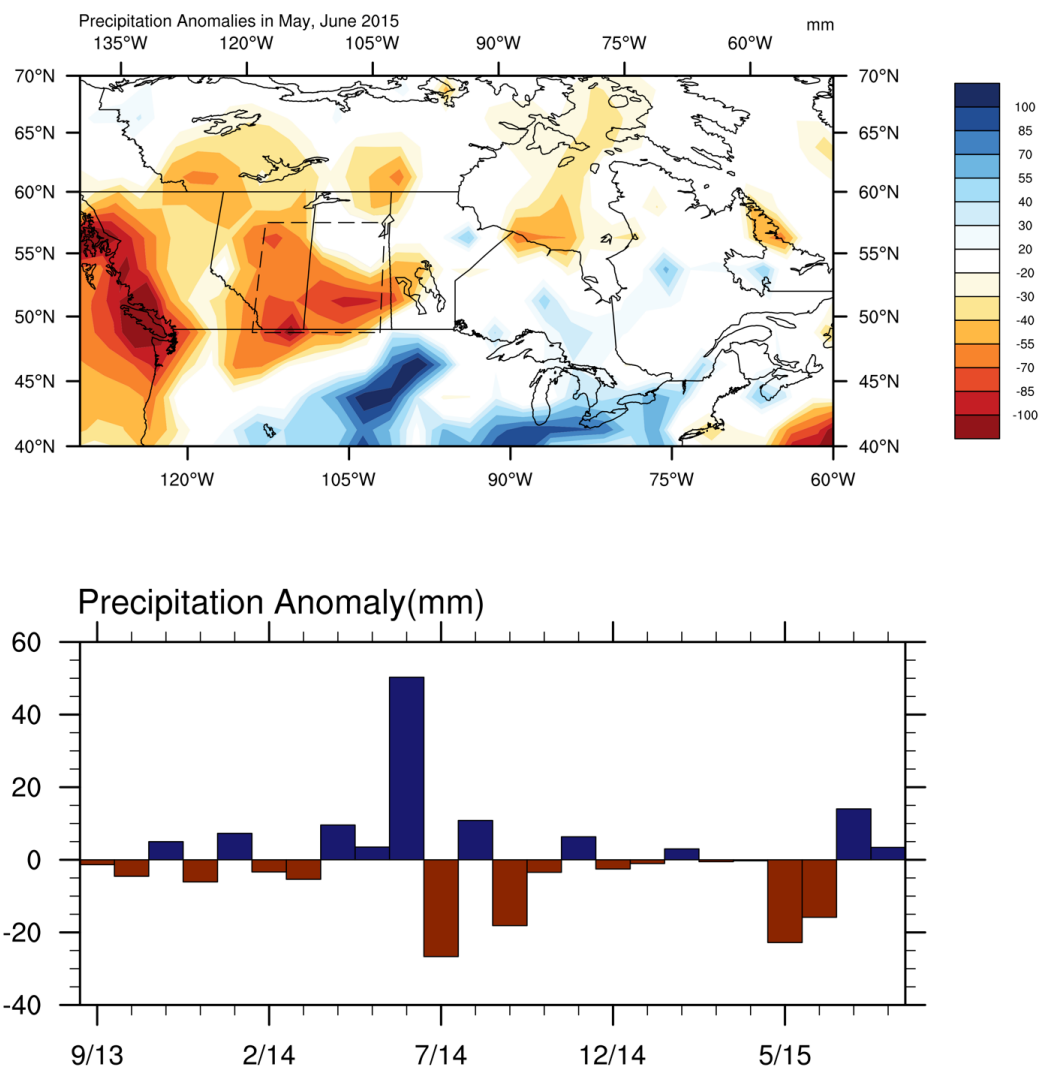
Fig. 1 Top: Precipitation anomalies (mm) from CMAP over the region (115 W-102.5 W, 50 N-57.5 N)

during May and June 2015. Bottom: time series of monthly precipitation anomaly over boxed region

between September 2013 and August 2015.

495
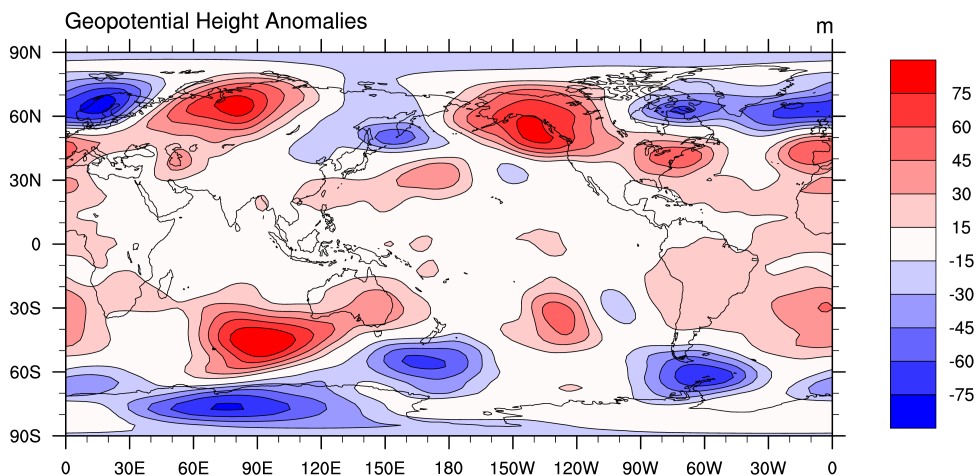
496

497 Fig. 2 NCEP GPH anomaly at 500hPa during May and June 2015 when the precipitation deficit was the

498 largest.

499

500

501

502

503

504

505

506

507

508
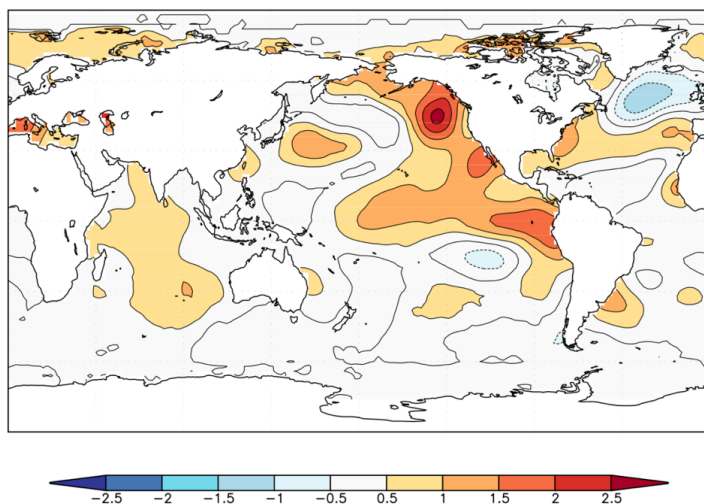
509

510   Fig. 3 The mean SST anomaly(℃) from ERSST v4 in May-August 2015.
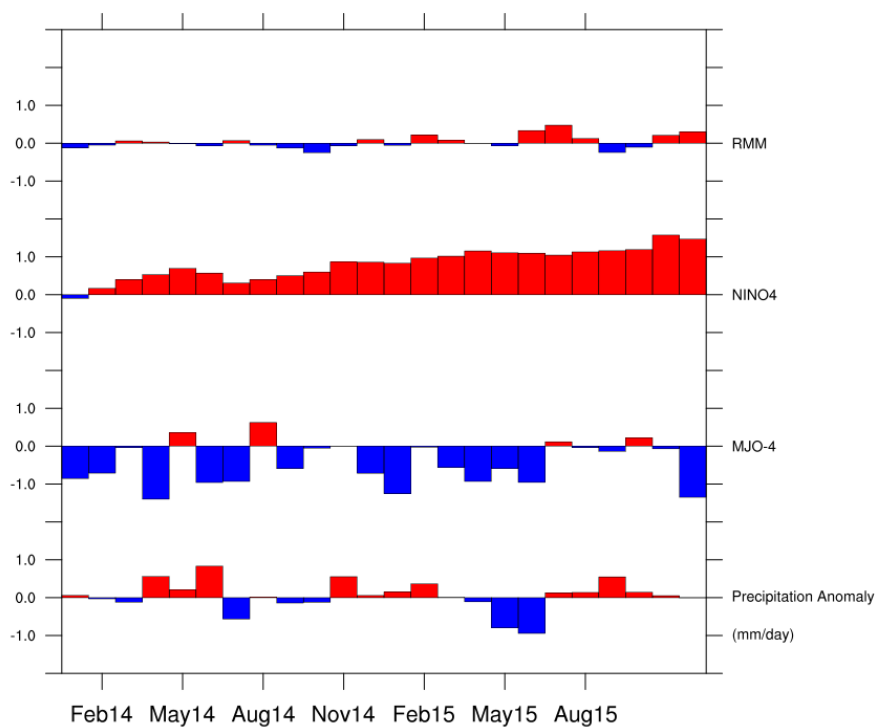
511

512 Fig. 4 RMM amplitude anomaly, NINO4, MJO 4 indices and precipitation anomaly of Canadian Prairies

513 from January 2014 to Dec 2015.

514

515

516

517

518

519
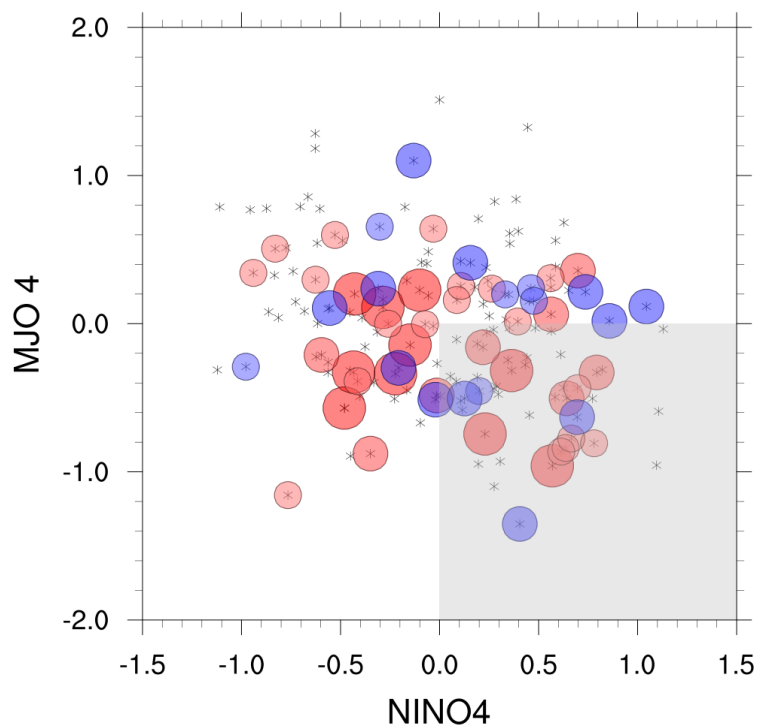
520

521   Fig. 5 The scatterplot of monthly precipitation anomaly (mm/month) as a function of MJO-4 and

522   NINO4. Each asterisk represents a month from May to August 1979-2016. Circled asterisk denotes a

523   month with precipitation anomaly larger than 18 mm/month. The blue circles are months with positive

524   precipitation anomaly and the red circles are months with negative precipitation anomaly. The sizes of

525   circles denote the magnitudes of the anomalies (large > 30 mm/month, medium > 24 mm/month,

526   small >18 mm/month). The shaded area denotes NINO4>0 and MJO-4 index < 0.

527
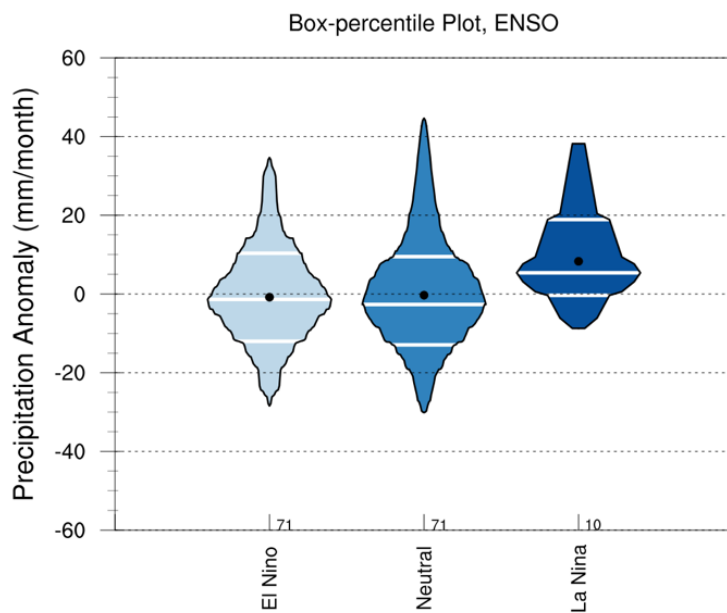
528

Fig. 6 The box-percentile plot of Canadian Prairies precipitation anomaly during growing season for

ENSO conditions.

531

532

533
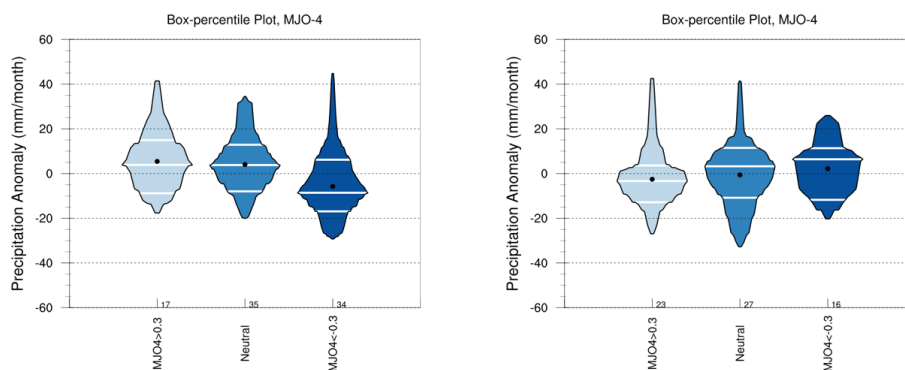
534

Fig. 7 Box-percentile plots of Canadian Prairies' precipitation anomaly during growing season

versus MJO-4 under warm NINO4 (NINO4> 0, left) and cold NINO4 (NINO4<0, right) condition.

537

538
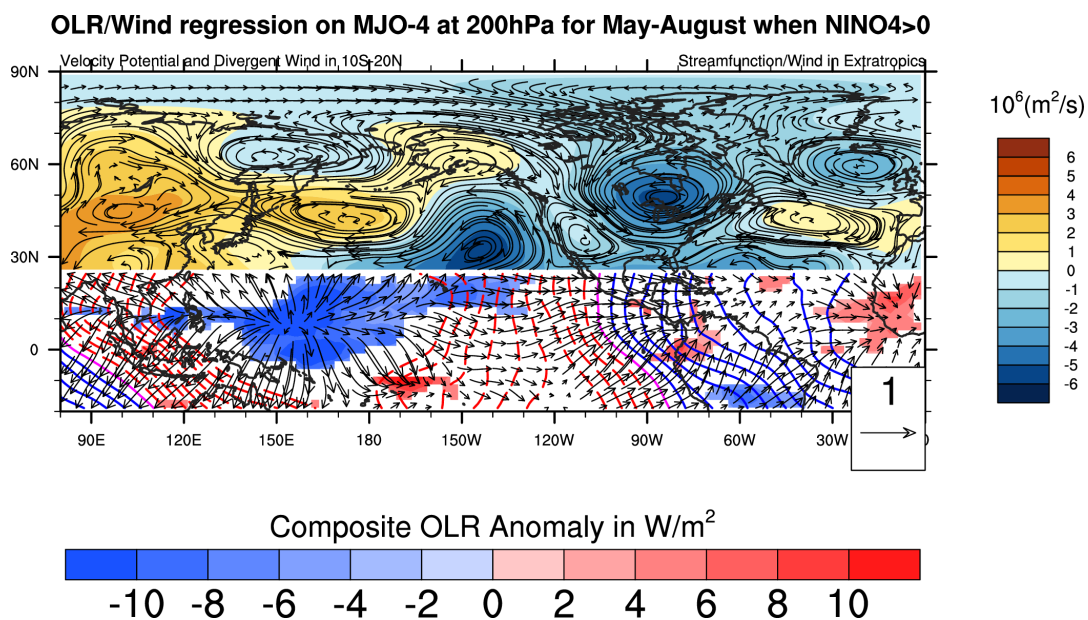
539

540

541    Fig. 8 The regression of stream function, wind field in the extratropics on MJO-4 for May-

542 August with MEI > 0.5. Bottom: OLR, velocity potential, and divergent wind in the tropics on MJO-4

543 indices for May-August with $NINO4 > 0$. The shaded region for the tropical OLR has p-value < 0.05.

544 Blue shading indicates active convection region. Red dashed contour and solid blue contour corresponds

545 to negative and positive velocity potential, respectively.

546

547

548